3D Invariants from Coded Projection without Explicit Correspondences

Kenta Suzuki, Fumihiko Sakaue and Jun Sato
Department of Computer Science, Nagoya Institute of Technology, Nagoya, Japan

Keywords: 3D Object Recognition, 3D Invariants, Projector-camera Systems, Coded-projection.

Abstract: In this paper, we propose a method for computing stable 3D features for 3D object recognition. The feature is projective invariant computed from 3D information which is based on disparity of two projectors. In our method, the disparity can be estimated just from image intensity without obtaining any explicit corresponding points. Thus, we do not need any image matching method in order to obtain corresponding points. This means that we can avoid any kind of problems arise from image matching essentially. Therefore, we can compute 3D invariant features from the 3D information reliably. The experimental results show our proposed invariant feature is useful for 3D object recognition.

1 INTRODUCTION

3D Object recognition is one of the most important problems in computer vision. The method can be applied to various kinds of applications, such as robot vision, visual surveillance and so on, and thus, the method is studied extensively(Murase and Nayar, 1995; Lowe, 1999; Hetzel et al., 2001; Toshev et al., 2009). The recognition method can be classified into two methods, that is appearance-based method(Murase and Nayar, 1995; Lowe, 1999) and 3D shape-based method(Hetzel et al., 2001; Toshev et al., 2009). The appearance based method is more familiar than shape-based method because we need only cameras in order to construct object recognition system. However, appearance of target object dramatically changes when viewpoint of camera is changed. Therefore, we need large number of images for achieving stable object recognition.

On the other hand, object shapes provide 3D information directly which is independent from view point. Thus, shape-based method is more stable than appearance-based method in general. However, we should obtain 3D information of target object by using some kind of sensors. In ordinary case, object shape is reconstructed from images taken by stereo cameras(Hartley and Zisserman, 2000). In this case, we first search corresponding points from stereo images. We next reconstruct object shape from the corresponding points. Although we can obtain 3D shape accurately when the corresponding points are correct, reconstructed shape is not correct if there are some incorrect corresponding points. Although many kinds of methods were proposed in order to find correct corresponding points, we cannot essentially avoid the corresponding problem in stereo camera systems, and wrong correspondences are always included in the results.

Another standard method for obtaining 3D shape is to use projector-camera systems(Caspi et al., 1998; Zhang et al., 2002; Vuylsteke and Oosterlinck, 1990; Proesmans et al., 1996; Boyer and Kak, 1987). In this method, feature points are projected onto target objects from a projector and the projected points are observed by a camera. By using the correspondences between projected point and observed point, we can reconstruct 3D shape as same as stereo camera systems. This method is preferable when we want to obtain object shape accurately because this active system is more stable than ordinary passive stereo camera systems. In addition, the system can reconstruct 3D shape even if a target object does not have any textures on surface of the object. However, the active system also suffers from wrong corresponding points if object texture is complex. Thus, we cannot avoid corresponding point problem again.

In order to avoid the wrong correspondence problem, Sakaue and Sato(Sakaue and Sato, 2011) proposed coded projection, which uses two projectors for recovering 3D shape of objects. In this method, we do not need to search corresponding points, and thus, we can essentially avoid the wrong correspondence problem in 3D shape recovery. However, their method is not sufficient to obtain accurate 3D shape because the main purpose of their method is not shape reconstruction but shape visualization, and, they did not con-

Suzuki K., Sakaue F. and Sato J..
3D Invariants from Coded Projection without Explicit Correspondences.
DOI: 10.5220/0004289802860293
In *Proceedings of the International Conference on Computer Vision Theory and Applications* (VISAPP-2013), pages 286-293
ISBN: 978-989-8565-48-8

Figure 1: Projected images. Intensities of red and green are horizontally varied and intensity of blue is fixed.

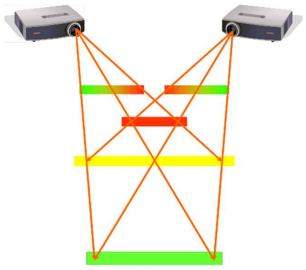

Figure 2: Coded projection from two projectors. Distance between projectors to object is visualized by color. Near objects from projectors are colored by red and far objects from projectors are colored by green.

sider reflectance property and normal direction of object surface. In this paper, we analyze the detail property of coded projection and propose a method for obtaining accurate and stable 3D information without any corresponding points search. Furthermore, we derive 3D invariants for 3D object recognition from measurement results.

2 VISUALIZATION OF DEPTH USING CODED PROJECTION

2.1 Depth Visualization

We first explain depth visualization by coded projection from multiple projectors(Sakaue and Sato, 2011). In this method, coded patterns are projected from two projectors to target objects simultaneously. Figure 1 shows projected patterns for depth visualization. In this image, intensities of red and green are horizontally varied and intensities of blue are fixed as follows:

$$\begin{cases} I_R = \frac{x}{W} \\ I_G = 1 - \frac{x}{W} \\ I_B = 0 \end{cases} \quad (0 \leq x \leq W) \qquad (1)$$

where I_R, I_G and I_B are intensities of each colors, x is horizontal axis, and W is the width of the image. The range of each intensity is $0 \sim 1$.

As shown in Fig. 2, the left projector projects Fig.1 and the right projector projects a reversed image. Then, projected images from the both projectors are combined on the surfaces of object in the scene.

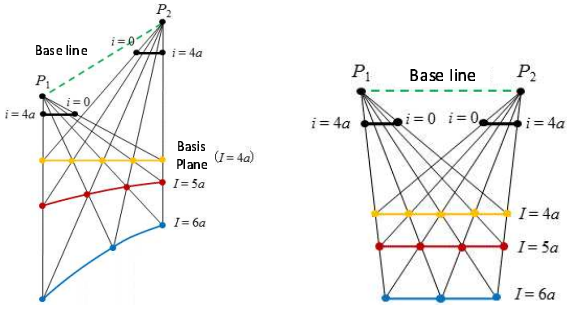

Figure 3: Distortion of depth visualization: Depth visualization is distorted when the base line and the basis plane is not parallel to each other as shown in Fig.(a). When the base line and the basis plane is parallel to each other, distortion of visualization.is eliminated.

As a result, depth of the scene is visualized as shown in Fig.2.

In this scene, near points are colored by red, middle points are colored by yellow and far points are colored by green. This visualization is caused by disparity of two projectors. For example, if the disparity is equal to zero, the projected images are completely overlapped, i.e., red colors lie onto green color and green colors lie onto red colors, and we can observe yellow colors. Therefore, we can visualize distance from projectors to a target as color information. The coloring of object point is based on the distance from yellow plane to the object point. We can change visualization of scene by controlling the plane. In this paper, we call the plane as basis plane for coded projection.

2.2 Arrangement of Basis Plane

In order to visualize depth information correctly, we have to parallelize the base line of two projectors and the basis plane. Let us consider a case where the base line is not parallel to the basis plane as shown in Fig.3(a). In this case, the depth visualization is distorted as shown by yellow, red and blue lines in Fig.3(a). On the other hand, if we arrange two projectors so that their base line is parallel to the basis plane, the depth visualization is not distorted as shown in Fig.3(b). Thus, in order to avoid the distortion problem, we should arrange the basis plane so that is is parallel to the base line of projectors.

2.3 Visualization of Various 3D Information

By changing the basis plane, we can visualize not only depth but also other information such as height.

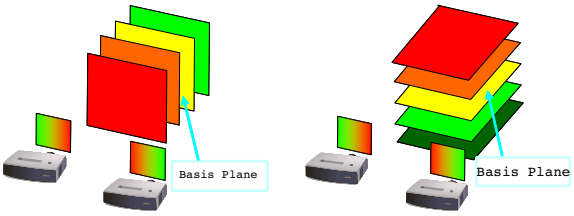

(a) Visualization of depth information.

(b) Visualization of height information.

Figure 4: Changes of visualized information depends on basis plane: We can control visualized information by changing the basis plane. In figure (a), depth from projectors is visualized. Height from the ground plane is visualized in figure (b). The change in visualization can be achieved by only changing the basis plane (yellow plane).

For example, depth from projectors are visualized by coded projection. In Fig.4(a), while the height from the ground plane is visualized in Fig.4(b). In order to change visualizing information, we should simply change direction of the basis plane. For example, we can visualize height when the basis plane is parallel to the ground plane.

As we showed in this section, the coded projection directly projects depth information to target object. Thus, we can avoid some important problems in stereo vision. First problem is the search of corresponding points. In ordinary stereo system, we should find corresponding point pair to estimate shape information. However, explicit corresponding points are not required in the coded projection because corresponding points in projected images are automatically combined and visualized by color on a target surface. Second, we do not need any computation to visualize depth because the depth is automatically represented by combination of projected image. Thus, there is no computational cost in the coded projection.

3 3D MEASUREMENT BY CODED PROJECTION

3.1 Depth Computation by Coded Projection

In the previous section, we showed depth visualization by using coded projection. In this section, we consider a method which can obtain accurate and stable 3D shape by using coded projection.

As shown in section **2**, the coded projection can visualize depth information by using color information. Thus, we can obtain depth information from image color. Let us consider a scene when two projectors are fixed in a scene. The projectors project coded

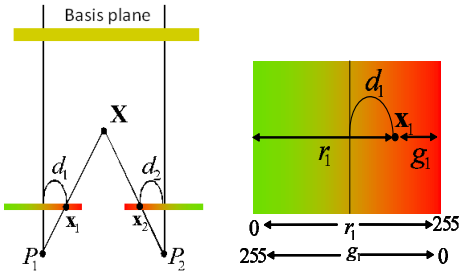

(a) (b)

Figure 5: Relationship between disparity and depth. Figure (a) indicates disparity d_1 and d_2 for a 3D point $\mathbf{X}$ and (b) indicates the relationship between color information and the disparity d.

patterns to target objects as shown in Fig. 5. In this case, we can represent disparity d of two projectors by using d_1 and d_2 as follows:

$$d = d_1 + d_2 \tag{2}$$

In general, depth D from projectors can be estimated by a disparity d as follows:

$$D = \frac{1}{d} \tag{3}$$

This equation indicates that we can estimate depth from disparity.

Under coded projection, we can simply obtain disparity between two projectors because color information directly represents disparity. Let us consider a scene as shown in Fig.5. In this scene, image points $\mathbf{x}_1$ and $\mathbf{x}_2$ are projected onto 3D point $\mathbf{X}$. Projected colors on a point $\mathbf{x}_1$ is described by r_1, g_1, and r_2, g_2 describe colors for point $\mathbf{x}_2$. In this case, irradiance R, G and B for $\mathbf{X}$ can be described as follows:

$$\begin{cases} R = r_1 + r_2 \\ G = g_1 + g_2 \\ B = 0 \end{cases} \tag{4}$$

From Eq.(1), r_1 and g_1 can be represented by d_1 as follows:

$$\begin{cases} r_1 = d_1 + 0.5 \\ g_1 = 0.5 - d_1 \end{cases} \tag{5}$$

Similarly, r_2 and g_2 can be described by d_2 as follows:

$$\begin{cases} r_2 = d_2 + 0.5 \\ g_2 = 0.5 - d_2 \end{cases} \tag{6}$$

From these equations, irradiance R, G and B can be rewritten as follows:

$$\begin{cases} R = d_1 + d_2 + 1 \\ G = 1 - (d_1 + d_2) \\ B = 0 \end{cases} \tag{7}$$

Thus, we can obtain a disparity d from colors as follows:

$$2d = 2(d_1 + d_2) = R - G \tag{8}$$

This equation indicates that we can measure object depth from irradiance of projectors. We do not need any complex method which provides corresponding points for stereo matching. We should only need to project coded image from projectors to a target object in order to obtain 3D information.

3.2 Irradiance Estimation from Images

We described a direct depth measuring method from projected irradiance in section **3.1**. The method has large advantage to ordinary stereo method because we can avoid correspondences problem in stereo matching. We, however, cannot obtain 3D information from ordinary input images because we can observe not irradiance but intensity from images. The intensity includes not only the effect of irradiance but also albedo, surface normal and so on. Thus, we have to extract magnitude of irradiance from input images to measure 3D information.

In general, most part of object surface can be approximately modeled by Lambertian surface model. We assume that reflectance model for all object surfaces can be represented by the Lambertian model. Therefore, observed intensities I_R, I_G and I_B on 3D point $\mathbf{X}$ illuminated by a projector $\mathbf{P}$ can be described as follows:

$$\begin{bmatrix} I_R \\ I_G \\ I_B \end{bmatrix} = \frac{\mathbf{n}^\top(\mathbf{X}-\mathbf{P})}{||\mathbf{X}-\mathbf{P}||^3} \begin{bmatrix} r\rho_R \\ g\rho_G \\ b\rho_B \end{bmatrix}, \tag{9}$$

where ρ_R, ρ_G, ρ_B and r, g and b denote albedo and irradiance for each channels, $\mathbf{n}$ and $\mathbf{P}$ indicate normal direction on a target surface and optical center of a projector. In this equation, $||\mathbf{X}-\mathbf{P}||$ indicates distance from a projector to an object surface and division by $||\mathbf{X}-\mathbf{P}||^2$ indicates irradiance attenuation by distance.

Equation(9) indicates that we have to know albedo of the surface, distance from projector and surface normal in order to estimate irradiance. Although estimation of these parameters from an input image is ill-posed problem, we can simply estimate these parameters from a particular image under a particular projected image. In this method, we can control lighting condition because light sources in the scene are projectors, and then, we can generate arbitrary lighting condition to obtain these parameters. Let us consider a case where a white image ($r = g = b = 1$) is projected by a projector. In this case, observed intensities I_{RW}, I_{GW} and I_{BW} can be represented as follows:

$$\begin{bmatrix} I_{RW} \\ I_{GW} \\ I_{BW} \end{bmatrix} = \frac{\mathbf{n}^\top(\mathbf{X}-\mathbf{P})}{||\mathbf{X}-\mathbf{P}||^3} \begin{bmatrix} \rho_R \\ \rho_G \\ \rho_B \end{bmatrix}. \tag{10}$$

If an optical center $\mathbf{P}$ is fixed, observed intensities directly represent effects of albedo, irradiance attenuation and normal direction in Eq.(9). Therefore, we can directly estimate irradiance in Eq.(9) as follows:

$$\begin{bmatrix} r \\ g \\ b \end{bmatrix} = \begin{bmatrix} I_R/I_{RW} \\ I_G/I_{GW} \\ I_B/I_{BW} \end{bmatrix}. \tag{11}$$

The estimation should be done for each projector, respectively. Then, depth D can be computed from irradiance r and g as follows:

$$D = \frac{2}{(r_1 + r_2) - (g_1 + g_2)} \tag{12}$$

where r_i and g_i denote irradiance of i-th projector estimated by Eq.(11).

4 PROJECTIVE INVARIANTS FOR 3D OBJECT RECOGNITION

4.1 3D Projective Invariants from Feature Points

From the estimated irradiance, we can obtain 3D information about target objects without explicitly obtaining stereo correspondences. It however includes projective ambiguity because relationship between two projectors is not explicitly calibrated. Therefore, we should consider this ambiguity to realize calibration-free 3D object recognition. In this section, we show two different methods to cope with this ambiguity.

We first explain a method which computes 3D projective invariants from 3D information. The cross ratio of 3D volumes is well known invariant under projective ambiguity. The invariant I can be estimated as follows:

$$I = \frac{|\widetilde{\mathbf{Y}}_1\widetilde{\mathbf{Y}}_2\widetilde{\mathbf{Y}}_3\widetilde{\mathbf{Y}}_4||\widetilde{\mathbf{Y}}_6\widetilde{\mathbf{Y}}_2\widetilde{\mathbf{Y}}_3\widetilde{\mathbf{Y}}_5|}{|\widetilde{\mathbf{Y}}_1\widetilde{\mathbf{Y}}_2\widetilde{\mathbf{Y}}_3\widetilde{\mathbf{Y}}_5||\widetilde{\mathbf{Y}}_6\widetilde{\mathbf{Y}}_2\widetilde{\mathbf{Y}}_3\widetilde{\mathbf{Y}}_4|}, \tag{13}$$

where $\mathbf{Y}_i$ indicate 3D information of i-th point under coded projection, which is computed from depth D_i and image point coordinate $\mathbf{x}_i$ as follows:

$$\mathbf{Y}_i = D_i\tilde{\mathbf{x}}_i \tag{14}$$

A symbol $\tilde{(\cdot)}$ denotes homogeneous representation. The invariant is independent from projective transformation of 3D scene, and thus, we can describe 3D objects uniquely even if measured information includes projective ambiguity.

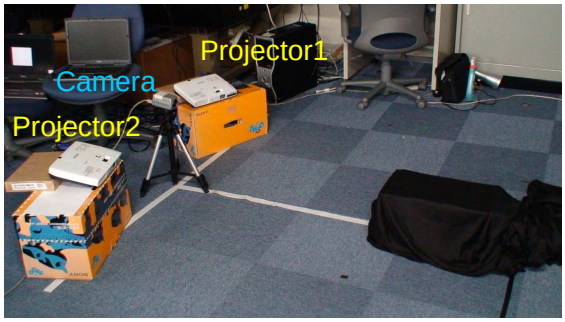

Figure 6: Experimental environment.

4.2 3D Invariant Image

The invariant described in previous section depends on image feature points. This invariant is very convenient when we can obtain sparse 3D information from input images. We however can obtain dense 3D information under coded projection easily, and thus, we should consider a method which uses dense information of images.

Under coded projection, complete depth map can be obtained up to projective ambiguity. Thus, we can transform images from a view point to another viewpoint by using projective transformation. A projective transformation $\mathbf{H}_{4\times4}$ can be described as follows:

$$\lambda\tilde{\mathbf{Y}}' = \mathbf{H}_{4\times4}\tilde{\mathbf{Y}}. \quad (15)$$

where λ denotes scale ambiguity, and, $\mathbf{Y}$ and $\mathbf{Y}'$ denote 3D points including projective ambiguity. The projective transformation can be estimated from 5 or more than 5 pairs of corresponding points. Then, we can transform all image points to another viewpoint by using the projective transformation. The transformed images are taken from the same viewpoint virtually, and thus, we can recognize the object by using ordinary 2D pattern recognition method without considering the difference in pose.

5 EXPERIMENTAL RESULTS

5.1 Environment

In this section, we show some experimental results from our proposed method. In these experiments, two projectors and a camera are fixed as shown in Fig.6. In this scene, a camera is fixed onto base line between two projectors. Coded patterns are projected from these projectors and target objects are illuminated by them. As a coded pattern for depth visualization, the image shown in Fig.1 was used. Target objects are shown in Fig.7. The objects are fixed on a stand in the experimental scene, and measured in 4 different poses, respectively. We show observed result and computed invariants in the next section.

(a) target(A) (b) target(B)

Figure 7: Target objects.

5.2 Measurement Results

Figure8 shows the result from coded projection for a target(A). The image (a) and (c) in Fig. 8 were taken under coded pattern and white pattern from projector1 respectively. As shown in image (a), the image intensity is affected by not only irradiance of projector but also albedo, normal direction and so on. On the other hand, image (c) includes only normal direction and albedo. From these images, image (e) was computed by Eq.(11). This image includes only irradiance because other components were eliminated by Eq.(11). Similarly, image (b) and (d) were taken under coded pattern and white pattern projected from projector2, and (f) is the estimated irradiance from (b) and (d). The image (g) is combined image of (e) and (f). In this image, subtractions of green from red components represent disparity between projector1 and projector2. For example near points from projectors, such as nose and foot, were colored by red. On the other hand, far points were colored by green. Finally, the image (h) represents depth from projectors computed by Eq.(3). In this image, near points are represented by dark intensity and far points are represented by bright intensity. From the disparity image, we can obtain 3D information without using any stereo matching method. Therefore, estimated depth is much more reliable than ordinary stereo reconstruction method based on feature point matching. In addition, we need very small computational cost for obtaining 3D information.

Note that, some points which has dark albedo cannot be measured correctly in this image because we cannot observe sufficient intensity onto the points. However, this disadvantage also exists on ordinary active stereo method because we cannot project/observe feature points onto darker pixels.

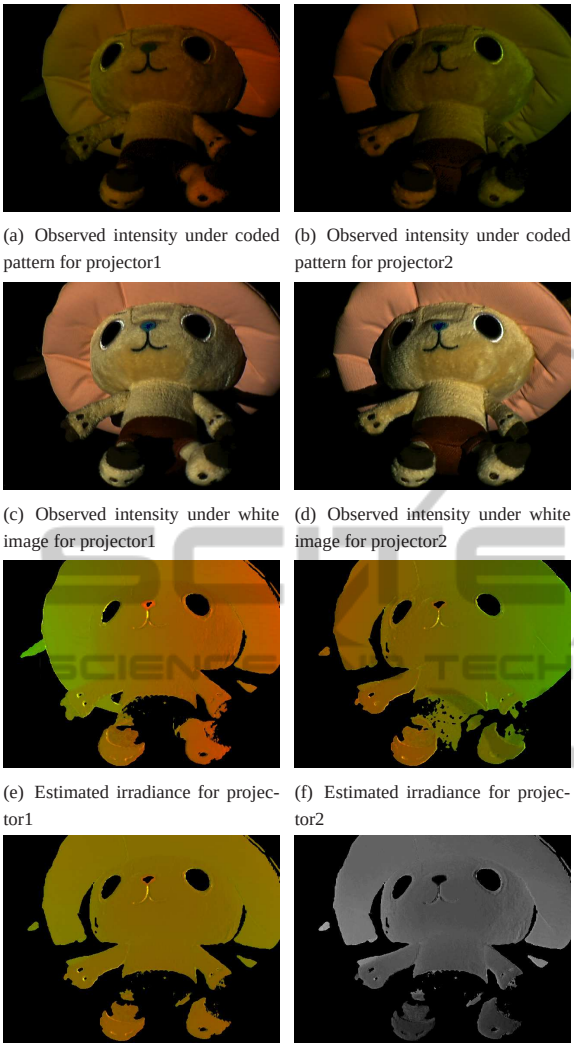

(a) Observed intensity under coded pattern for projector1

(b) Observed intensity under coded pattern for projector2

(c) Observed intensity under white image for projector1

(d) Observed intensity under white image for projector2

(e) Estimated irradiance for projector1

(f) Estimated irradiance for projector2

(g) Colored disparity image

(h) Depth image

Figure 8: Measured results under coded projections. Image (a) and (b) were taken under coded pattern from projector1 and 2, (c) and (d) were taken under white pattern, and, (e) and (f) are estimated irradiance. The image (g) is a combined image of (e) and (f), and the image (h) is a depth map computed from the inverse of image (g).

5.3 3D Invariants from Images

We next show 3D invariants estimated from Fig.8(h) by using the proposed method. At first, we show 3D invariant images described in section **4.2**. In this experiment, we measured a target object in different poses. One of the measured result is shown in Fig.9 (a) and (b). Figure9(a) shows an image taken under white projection, and Fig.9(b) shows a measured depth. The results from another pose are shown in Fig.9 (c) and (d). In image (a) and image (c), feature point pairs were extracted by SIFT(Lowe, 1999),

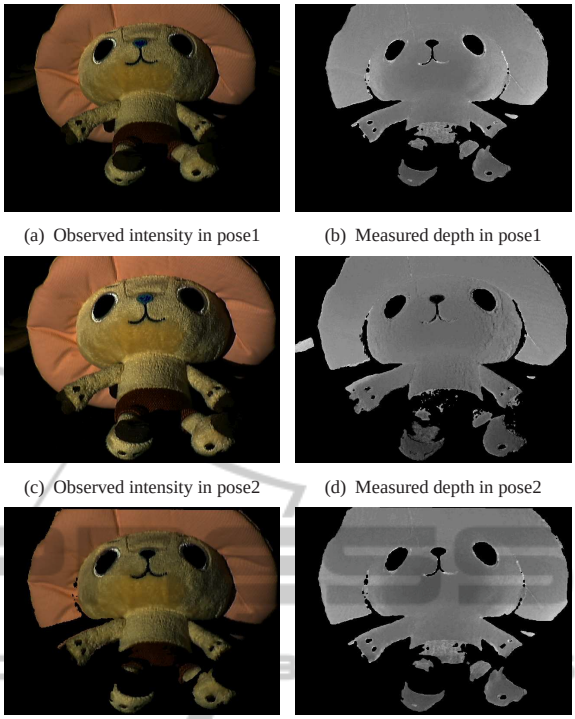

(a) Observed intensity in pose1

(b) Measured depth in pose1

(c) Observed intensity in pose2

(d) Measured depth in pose2

(e) Transformed image

(f) Transformed depth

Figure 9: Virtual viewpoint transformation: Images (a) and (b) are images taken under white projection and a measured depth in pose1. Images (c) and (d) are those in pose2. Image (e) and (f) show image intensity and depth in pose2 transformed from pose1.

Table 1: Deference of invariants on each pose.

	pose2	pose3	pose4
Difference of 3D invariant	0.002	0.027	0.044

and then, projective transformation in Eq.(15) was estimated by using the point pairs of depth map(b) and (d). By using the estimated transformation and depth images, image (a) and (b) were transformed to image (e) and (f) whose pose coincides with that of image (c) and (d) on pose 2. Although the original images (a) and (c) are different from each other, the transformed image (e) is almost identical with (c), and we can use them for recognizing objects under different viewpoints. Figure 10 shows results from target (B). As shown in these figures, we can also virtually transform images from a viewpoint to another viewpoint by our proposed method. We next show point-based 3D invariant computed by Eq. (13). At first target A was measured in 4 different poses and corresponding points were extracted by SIFT as same as the previous experiment. By using the points, 3D invariants were computed in each pose. Table 1 shows difference of invariants from pose1 to another pose.

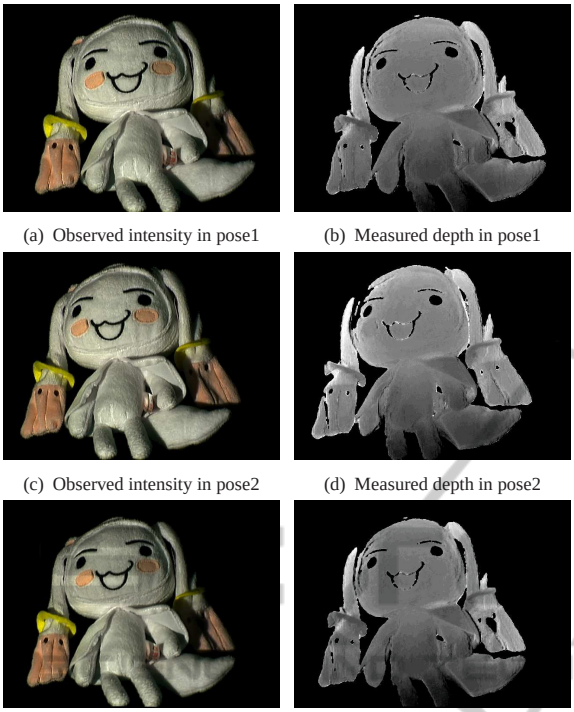

(a) Observed intensity in pose1 (b) Measured depth in pose1

(c) Observed intensity in pose2 (d) Measured depth in pose2

(e) Transformed image (f) Transformed depth

Figure 10: Virtual viewpoint transformation: Images (a) and (b) are images taken under white projection and a measured depth in pose1. Images (c) and (d) are those in pose2. Image (e) and (f) show image intensity and depth in pose2 transformed from pose1.

Table 2: Deference of invariants in each pose.

(A) \(B)	pose1	pose2	pose3	pose4
pose1	27.722	4.380	-	-
pose2	0.338	0.308	0.407	-
pose3	0.041	0.180	-	-
pose4	-	-	-	-

The table shows that our proposed invariants can provide similar value even if measured objects have different poses.

We next show difference of 3D invariants for different objects. In this experiment, target (A) and target (B) was measured in 4 different poses and corresponding points were extracted by SIFT in images. By using the points, 3D invariants were computed. The difference of the invariants are shown in table 2. In this table, a value of i-th row in j-th column indicates difference of 3D invariants between target (A) in pose-i and target (B) in pose-j. In addition, "-" indicates that we cannot extract corresponding point from the image pair. In this table, almost all the difference of 3D invariants are larger than those in table1. The fact indicates that our proposed invariants can distinguish objects even if object poses are different each other.

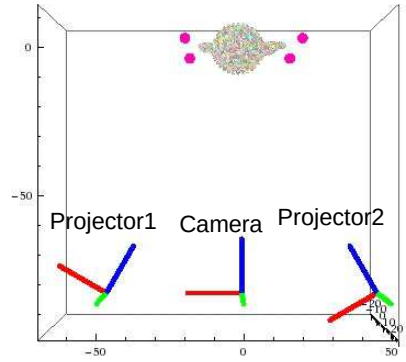

Figure 11: Synthesized environment: Red, green and blue axis for a camera and projectors indicate optical axes of them. Red points around a target object indicate basis plane used for generating coded projector patterns.

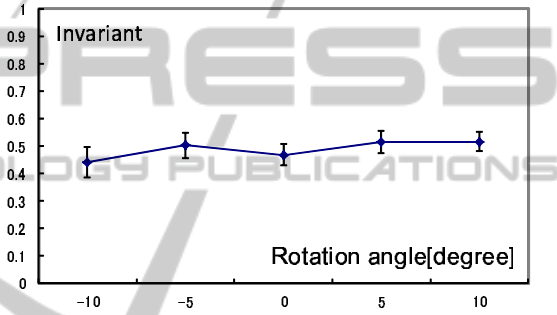

Figure 12: Relationship between object pose and 3D invariant. Horizontal axis indicates rotation angle of an object and vertical axis indicates 3D invariant.

5.4 Stability Evaluation

We next show the stability of the proposed method by using synthesized data. In this experiment, two projectors, a camera and a target object are arranged as shown in Fig.11. The coded projection was observed by the camera, and random intensity noise with STD of 1.0 were added to the observed image.

The target object was rotated at the same position, and, the 3D invariant described in Eq. (13) was computed in each pose. Figure 8 shows computed invariants in each pose. The figure indicates that computed invariants are stable even if pose of an object is changed.

Figure 13 shows 3D invariant when the base line length between two projectors was changed. In this experiment, distance between two projectors was changed from 40cm to 100cm. Under each base line length, 3D invariants were computed for each pose. Figure13 indicates that our proposed invariants are almost identical even if the base line length between two projector was changed. The facts indicate that our proposed method is robust against changing pose and changing projectors positions.

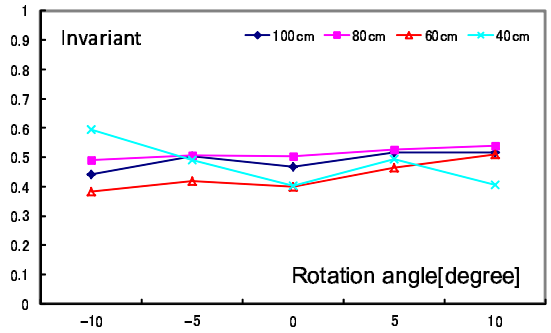

Figure 13: Relationship between base line length and 3D invariants.

6 CONCLUSIONS

In this paper, we proposed a 3D measurement method based on disparity between two projectors. In this method, we do not need to search image corresponding points, and thus, we can avoid various kind of problems such as wrong correspondences and computational cost. In addition, we proposed method for deriving 3D features which are invariant under projective ambiguity. We finally presented some experimental results and showed that our proposed method is useful for 3D object recognition.

REFERENCES

Boyer, K. L. and Kak, A. C. (1987). Color-encoded structured light for rapid active ranging. *IEEE Trans. Pattern Anal. Mach. Intell.*, 9(1):14–28.

Caspi, D., Kiryati, N., and Shamir, J. (1998). Range imaging with adaptive color structured light. *IEEE Trans. Pattern Anal. Mach. Intell.*, 20(5):470–480.

Hartley, R. and Zisserman, A. (2000). *Multiple View Geometry in Computer Vision*. Cambridge University Press.

Hetzel, G., Leibe, B., Levi, P., and Schiele, B. (2001). 3d object recognition from range images using local feature histograms. In *CVPR (2)'01*, pages 394–399.

Lowe, D. G. (1999). Object recognition from local scale-invariant features. In *Proc. of the International Conference on Computer Vision, Corfu*.

Murase, H. and Nayar, S. K. (1995). Visual learning and recognition of 3-d objects from appearance. *International Journal of Computer Vision*, 14:5–24.

Proesmans, M., Van Gool, L., and Oosterlinck, A. (1996). One-shot active 3d shape acquisition. In *Proceedings of the International Conference on Pattern Recognition (ICPR '96) Volume III-Volume 7276 - Volume 7276*, ICPR '96, pages 336–, Washington, DC, USA. IEEE Computer Society.

Sakaue, F. and Sato, J. (2011). Surface depth computation and representation from multiple coded projector light. In *Proc. IEEE International Workshop on Projector-Camera Systems (PROCAMS2011)*, pages 75–80.

Toshev, A., Makadia, A., and Daniilidis, K. (2009). Shape-based object recognition in videos using 3d synthetic object models. In *CVPR*, pages 288–295.

Vuylsteke, P. and Oosterlinck, A. (1990). Range image acquisition with a single binary-encoded light pattern. *IEEE Trans. Pattern Anal. Mach. Intell.*, 12(2):148–164.

Zhang, L., Curless, B., and Seitz, S. M. (2002). Rapid shape acquisition using color structured light and multi-pass dynamic programming. In *The 1st IEEE International Symposium on 3D Data Processing, Visualization, and Transmission*, pages 24–36.